Supporting Information

Chemosensor for micro to nano-molar detection of Ag^{+} and Hg^{2+} ions in pure aqueous media and its applications in cell imaging

Jitendra P. Nandre[a], Samadhan R. Patil[a], Suban K. Sahoo[c], Chullikkattil P. Pradeep[d], Andrei Churakov[e], Fabiao Yu[f], Lingxin Chen*[f], Carl Redshaw[g], Ashok A. Patil[a]*, Umesh D. Patil*[b]

[a]*Department of Chemistry, Z. B. Patil College, Deopur, Dhule - 424 002 (MS), India.*

[b]*Department of Chemistry, S.S.V.P.S's L. K. Dr. P. R. Ghogrey Science College, Dhule-424 001 (MS), India.*

[c]*Department of Applied Chemistry, S. V. National Institute Technology, Surat-395007, Gujrat, India.*

[d]*School of Basic Sciences, Indian Institute of Technology Mandi, Mandi, Himachal Pradesh, 175001, India.*

[e]*Institute of General and Inorganic Chemistry, Russian Academy of Sciences, Leninskii prosp. 31, Moscow 119991, Russian Federation.*

[f]*Key Laboratory of Coastal Zone Environmental Processes and Ecological Remediation, Yantai Institute of Coastal Zone Research, Chinese Academy of Sciences, Yantai 264003, China*

[g]*Department of Chemistry, University of Hull, Cottingham Road, Hull, HU6 7RX (UK).*

Table of Contents

Experimental Section

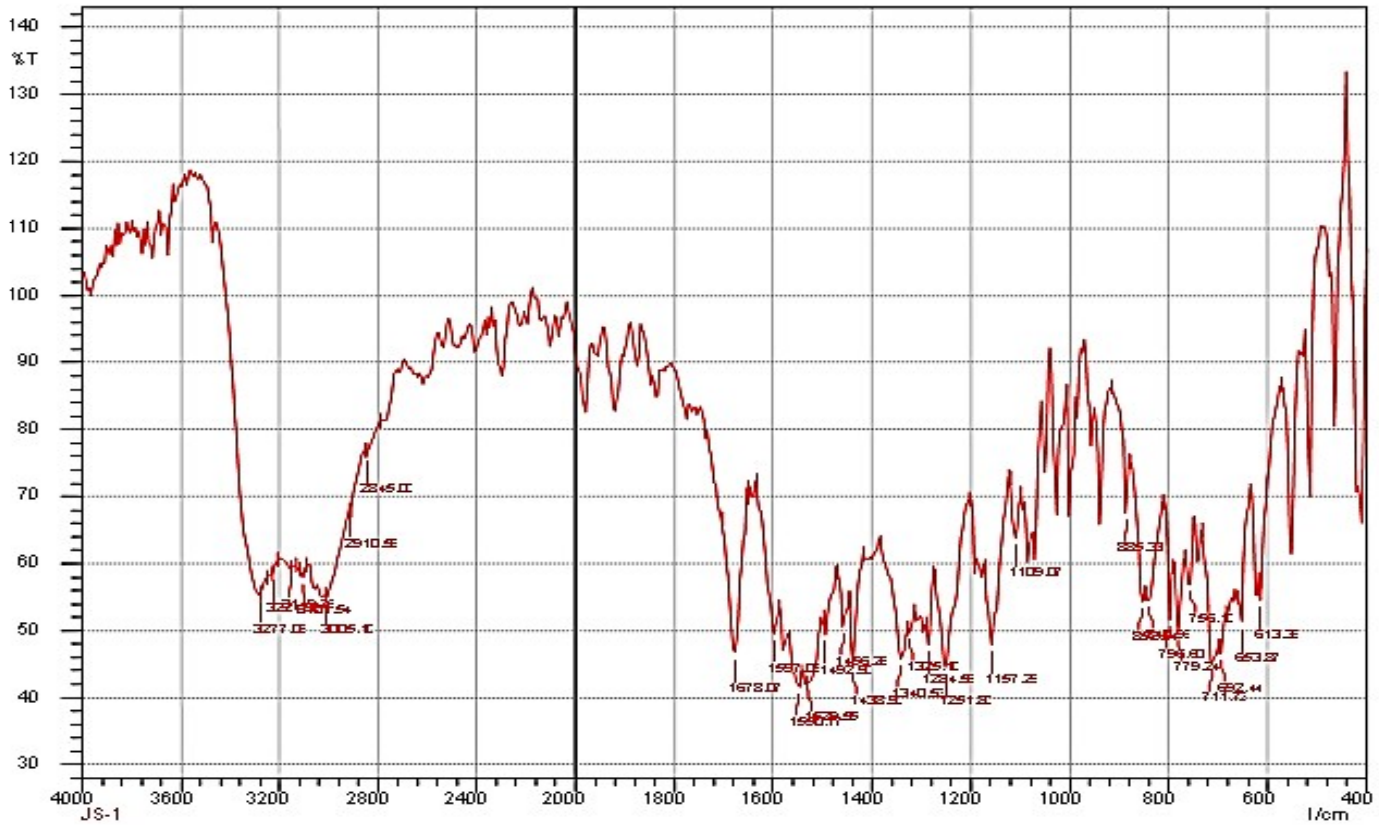

Figure S-1: FT-IR spectrum of sensor **PTB-1**.

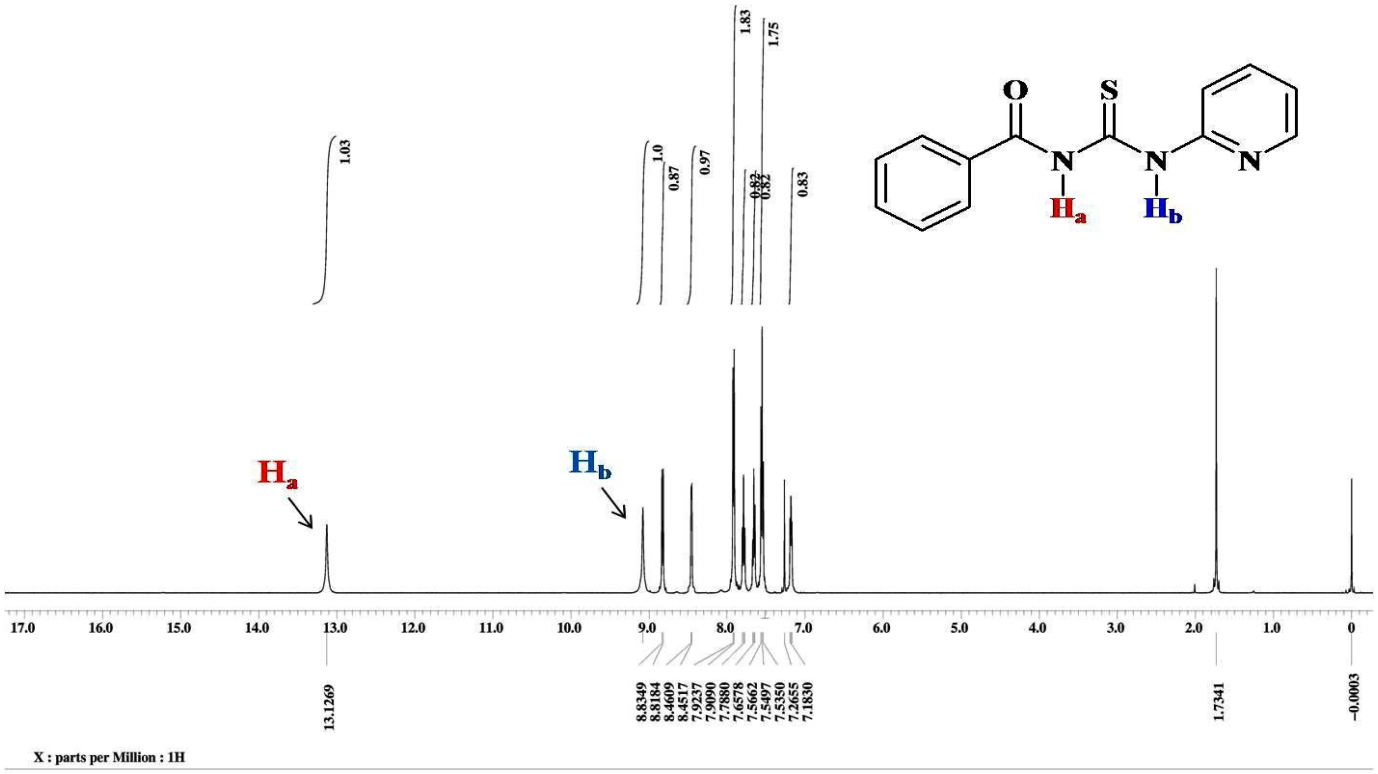

Figure S-2: ^{1}H-NMR spectrum of sensor **PTB-1**.

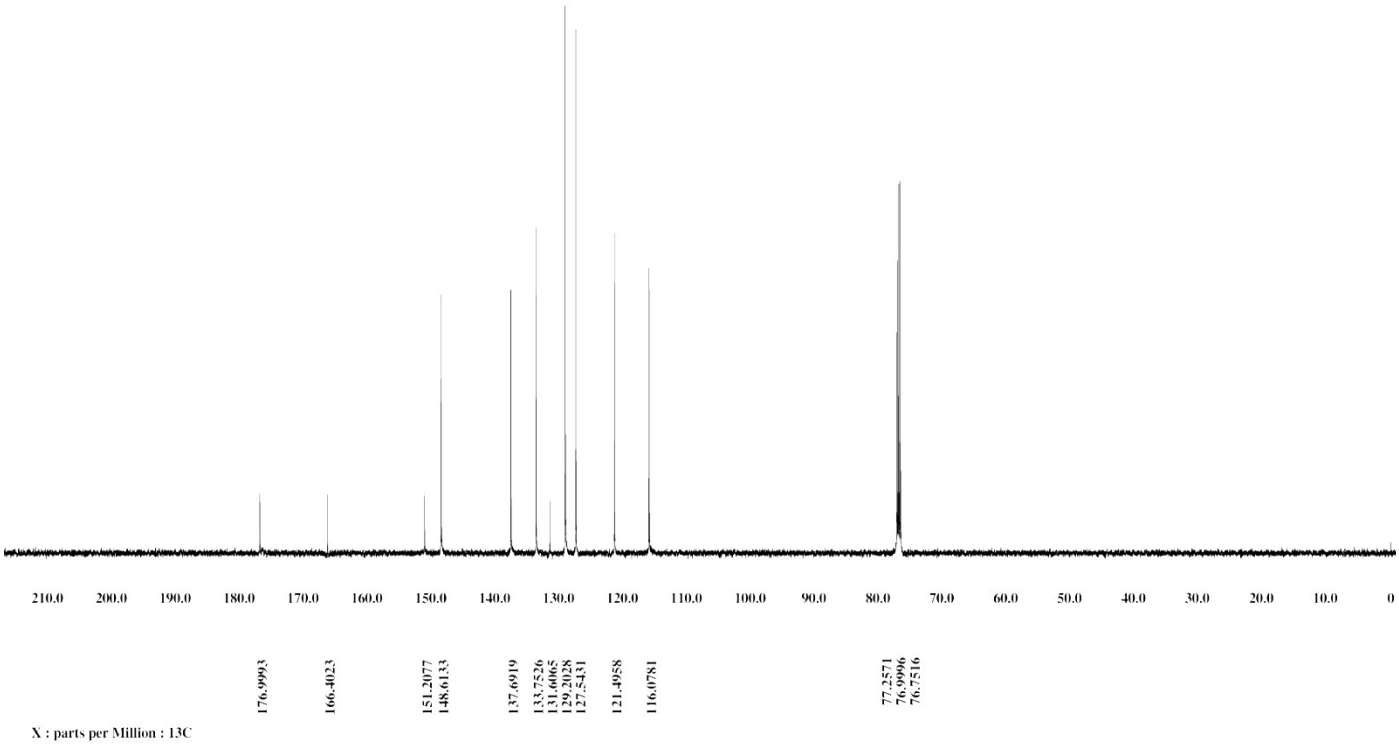

Figure S-3: ^{13}C-NMR spectrum of sensor **PTB-1**

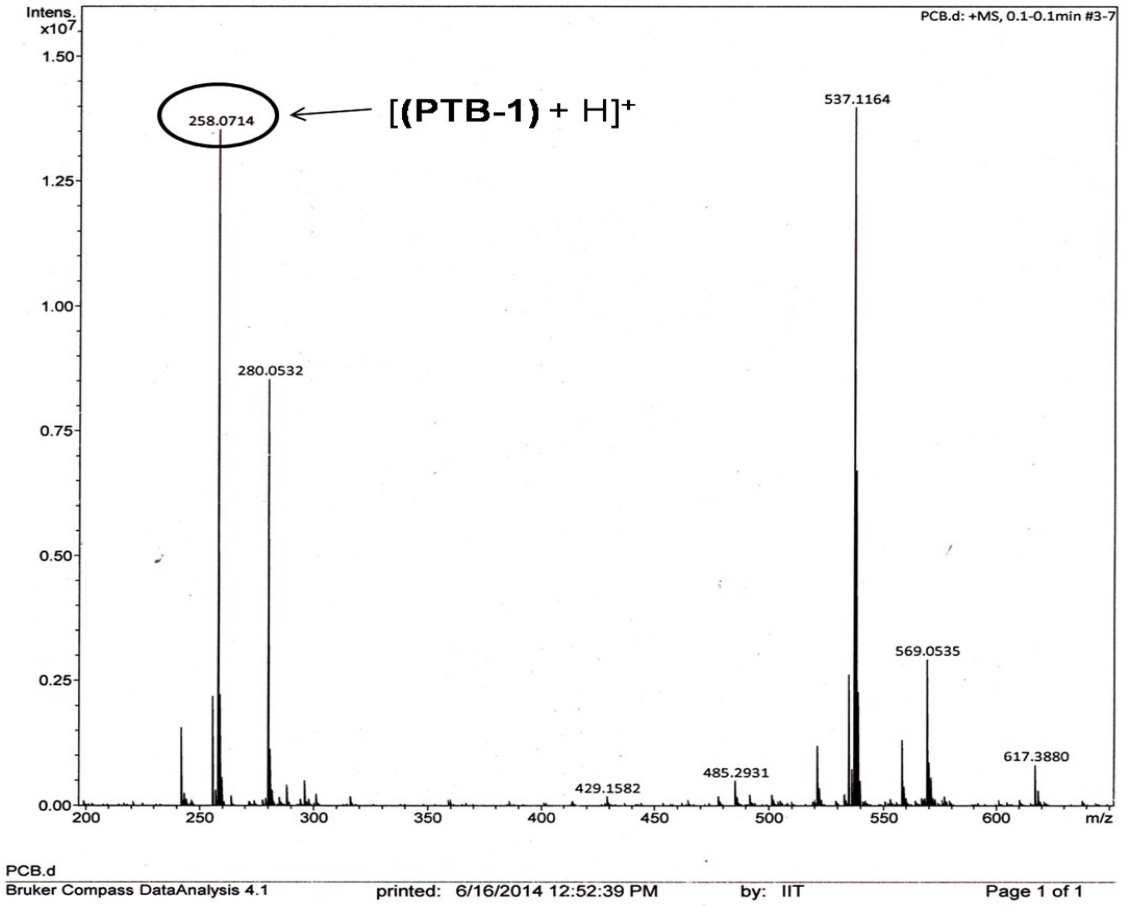

Figure S-4: HRMS spectrum of sensor **PTB-1**.

Figure S-5: Concentration dependent naked-eye study; 2 equivalents of Ag^+ ions of concentrations (**A)** Ag^+ (5 x 10^{-3} M); (**B)** Ag^+ (1 x 10^{-3} M); (**C)** Ag^+ (5 x 10^{-4} M); (**D)** Ag^+ (1 x 10^{-4} M); (**E)** Ag^+ (1 x 10^{-5} M) in the presence of 1 equivalent of **PTB-1** (5 x 10^{-3} M).

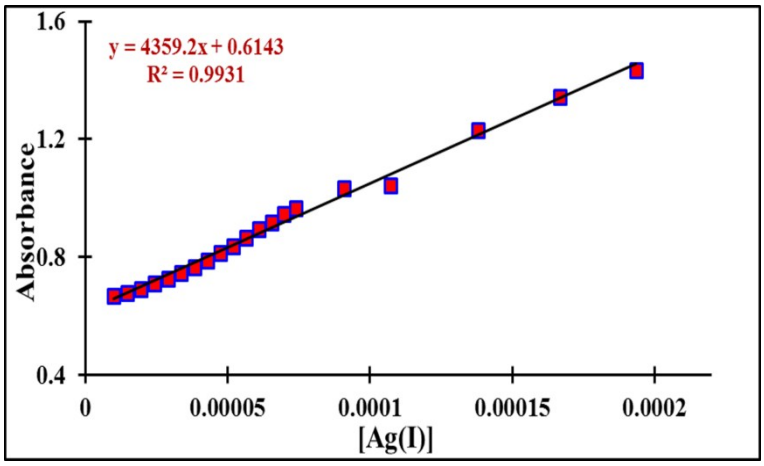

Figure S-6: Linear fitting curve for LOD and LOQ determination of **PTB-1** for Ag^+.

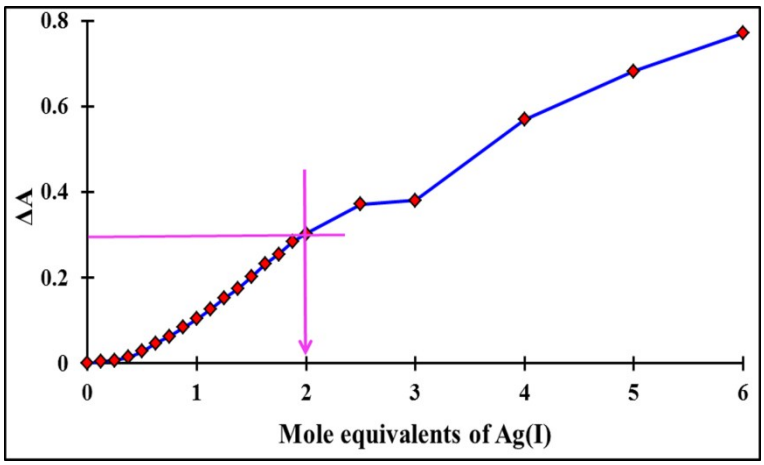

Figure S-7: Mole ratio plot/change in absorption spectra (ΔA) as a function of concentration of Ag^+ ions.

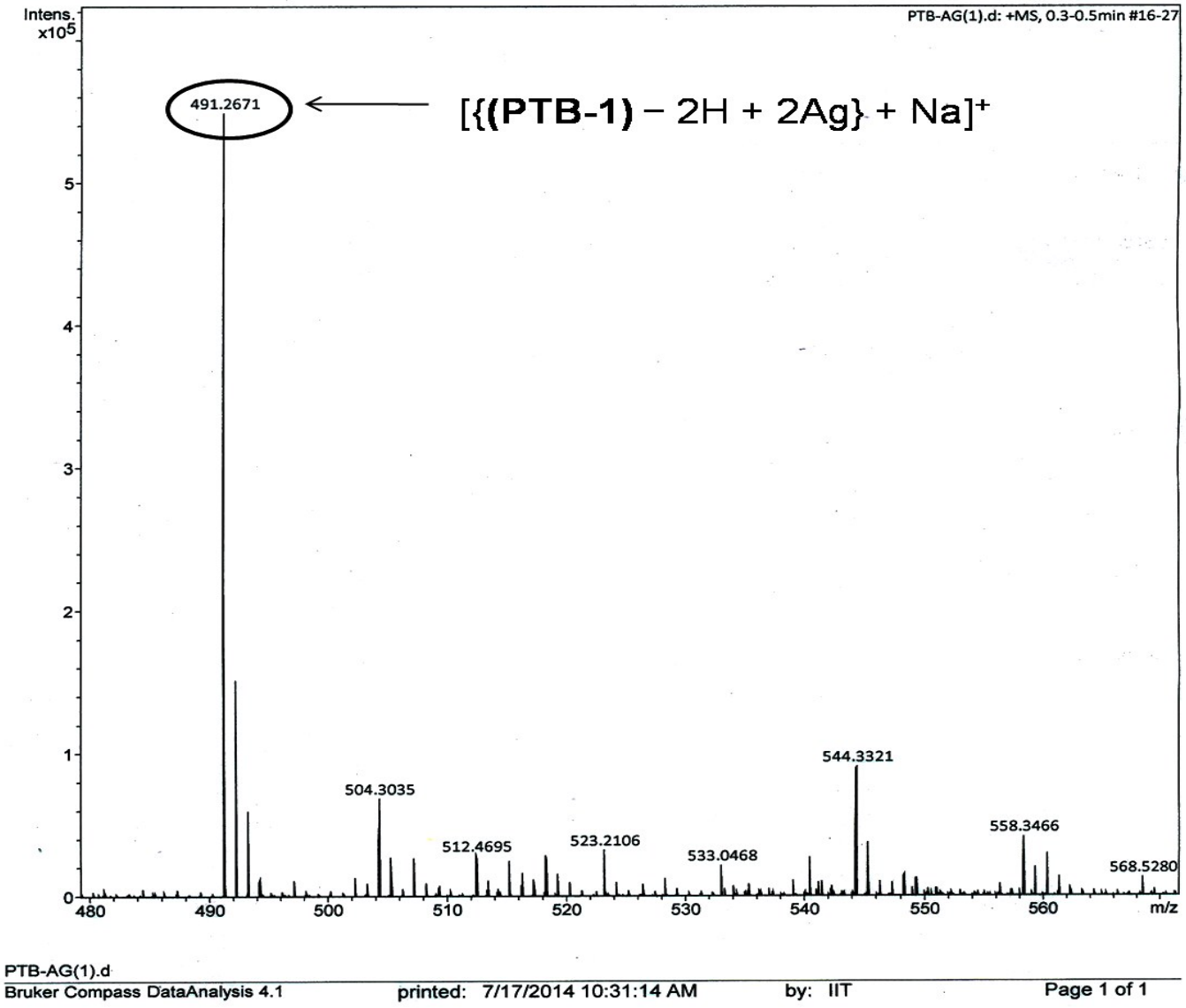

Figure S-8: Mass spectrum of **PTB-1** in the presence of Ag^{+}.

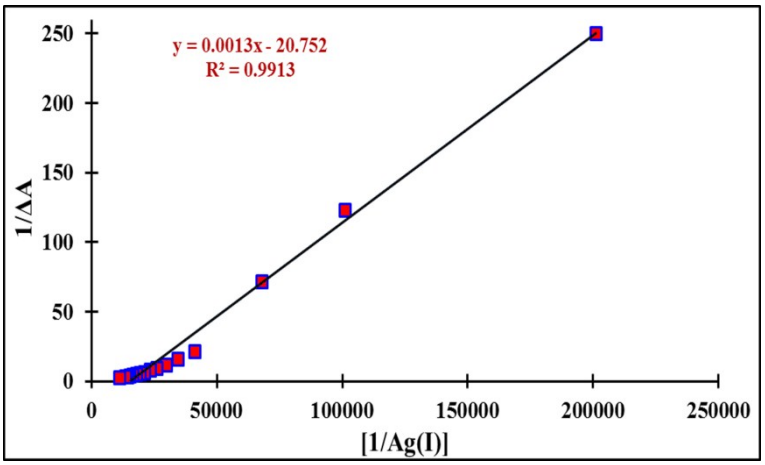

Figure S-9: Benesi-Hildebrand plot of 1/ ΔA against 1 / [Ag^{+}].

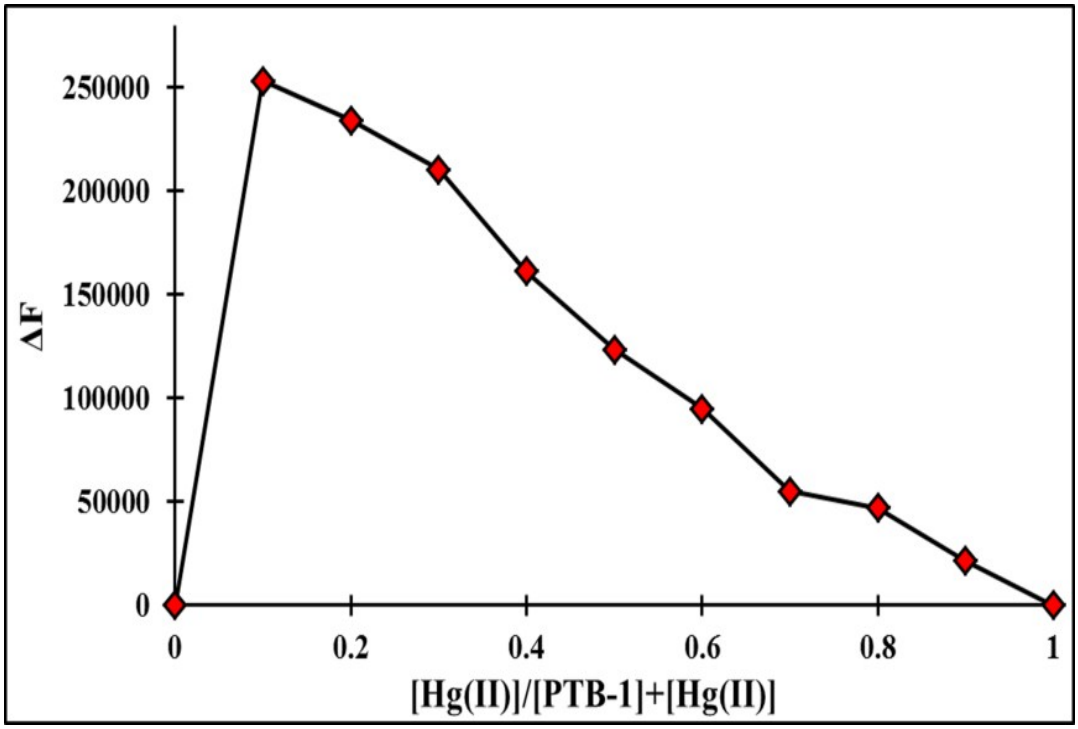

Figure S-10: Job's plot for the determination of the 2:1 stoichiometry for complexation of **PTB-1** with Hg^{2+} ion.

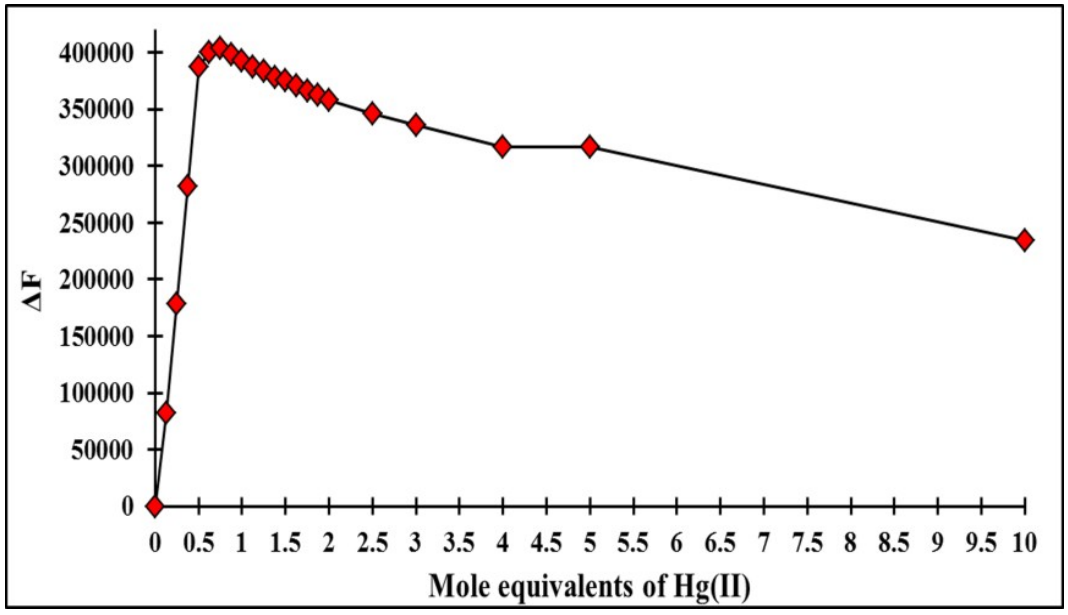

Figure S-11: Mole ratio plot/change in emission spectra (ΔF) as a function of concentration of Hg^{2+} ion.

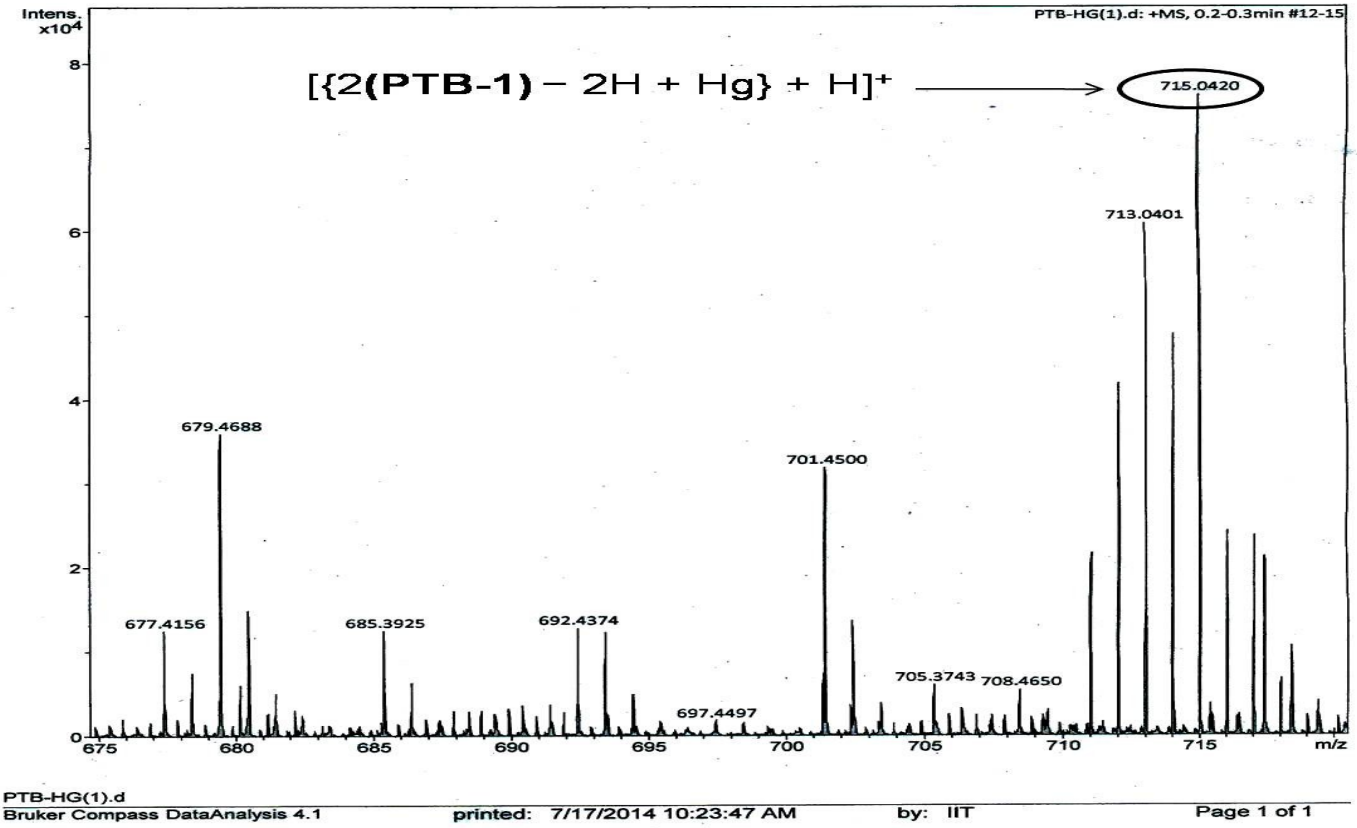

Figure S-12: Mass spectrum of **PTB-1** in the presence of Hg^{2+}.

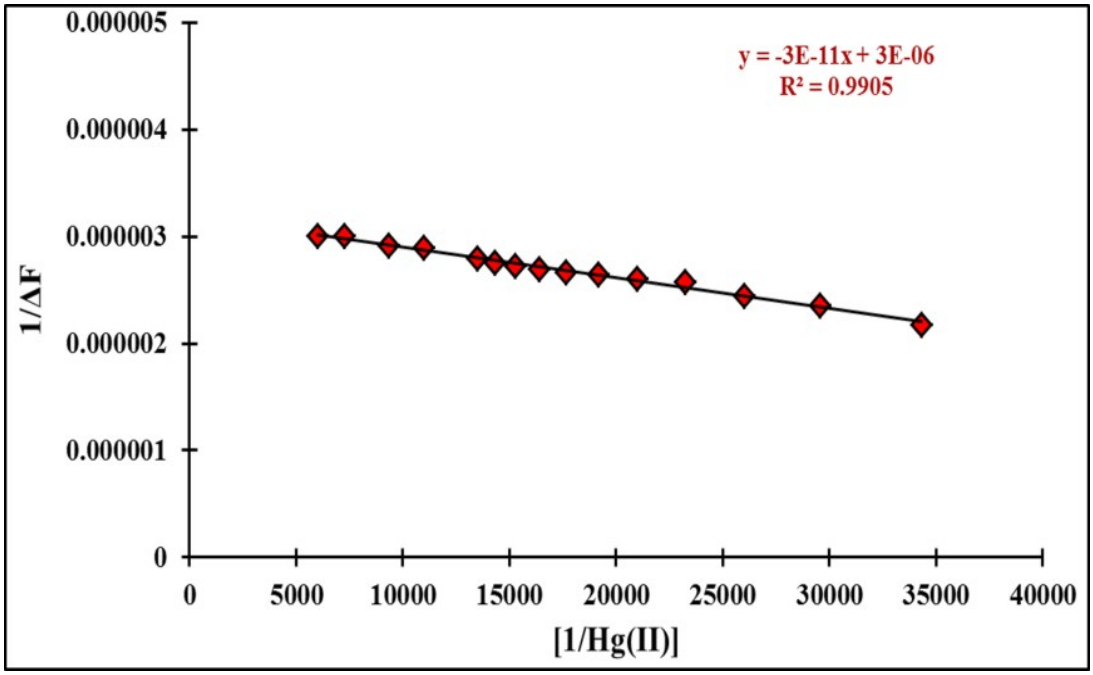

Figure S-13: Benesi-Hildebrand plot of 1/ ΔF against 1 / [Hg^{2+}].

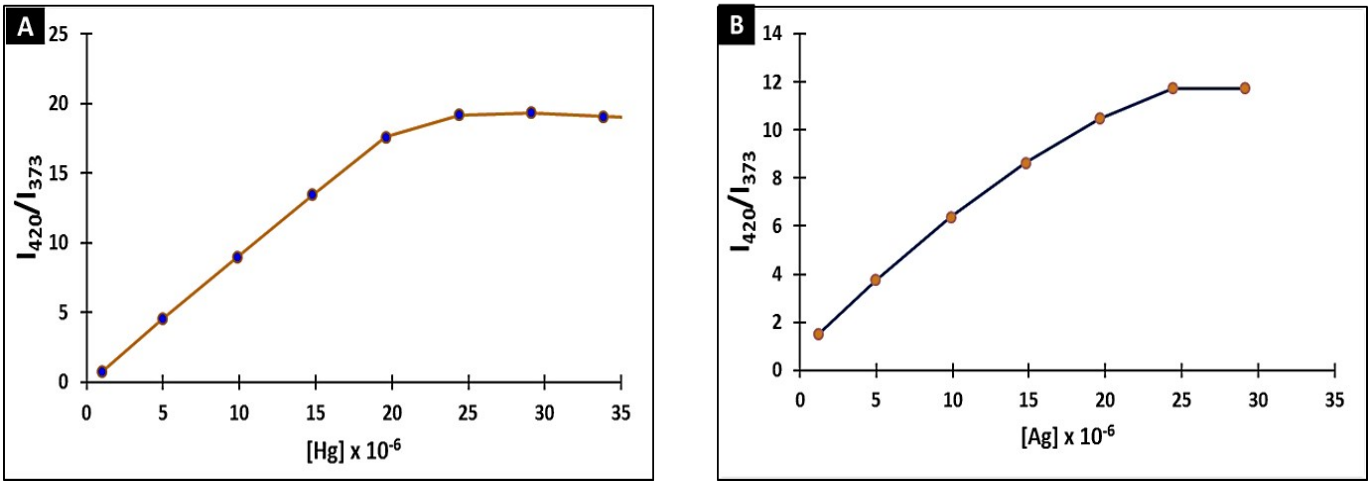

Figure S14: Plots of the fluorescence intensity of PTB-1 vs. the increasing concentration of (A) Hg^{2+} and (B) Ag^{+}.

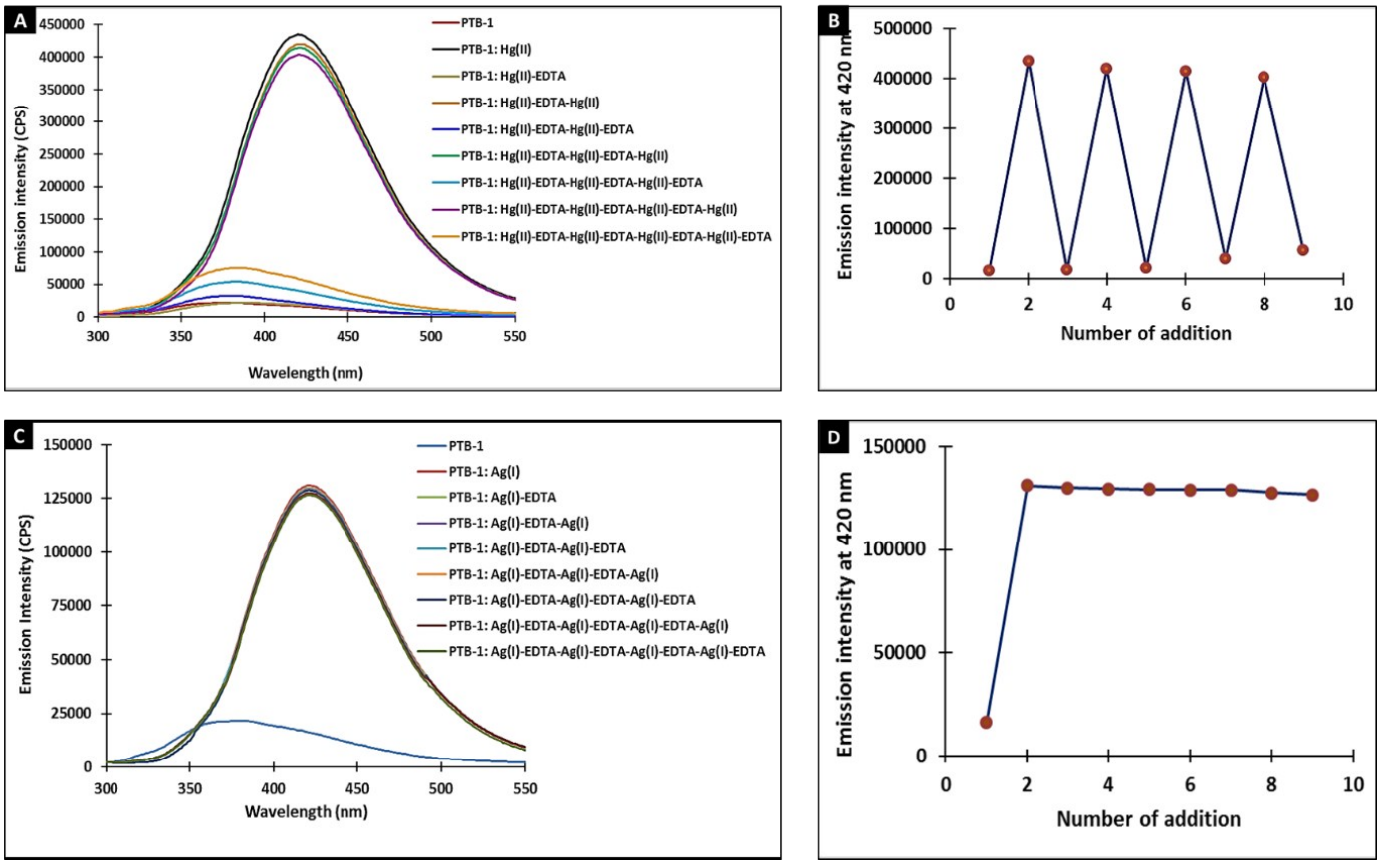

Figure S15: Selectivity and reversibility measurement of PTB-1 to Hg^{2+} and Ag^{+}.

Changes in fluorescence emission intensity of PTB-1 [2 mL, 4 x 10^{-5} M, in CH_3OH:H_2O (20:80, v/v)] upon the sequential addition of (A, B) Hg^{2+} and EDTA; (C, D) Ag^{+} and EDTA at λ_{ex} = 290 nm.

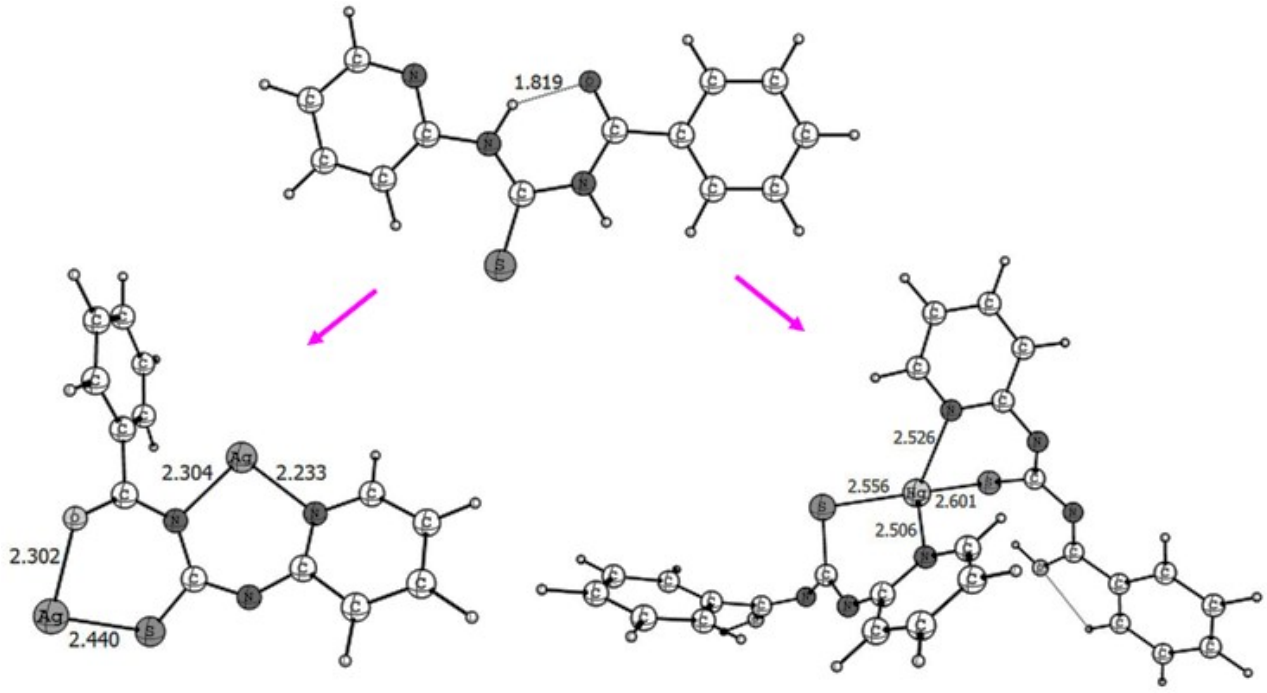

Figure S16: The DFT computed molecular structure of **PTB-1** and its **PTB-1.**$(Ag^{+})_2$ and $(\mathbf{PTB\text{-}1})_2.Hg^{2+}$ complexes.

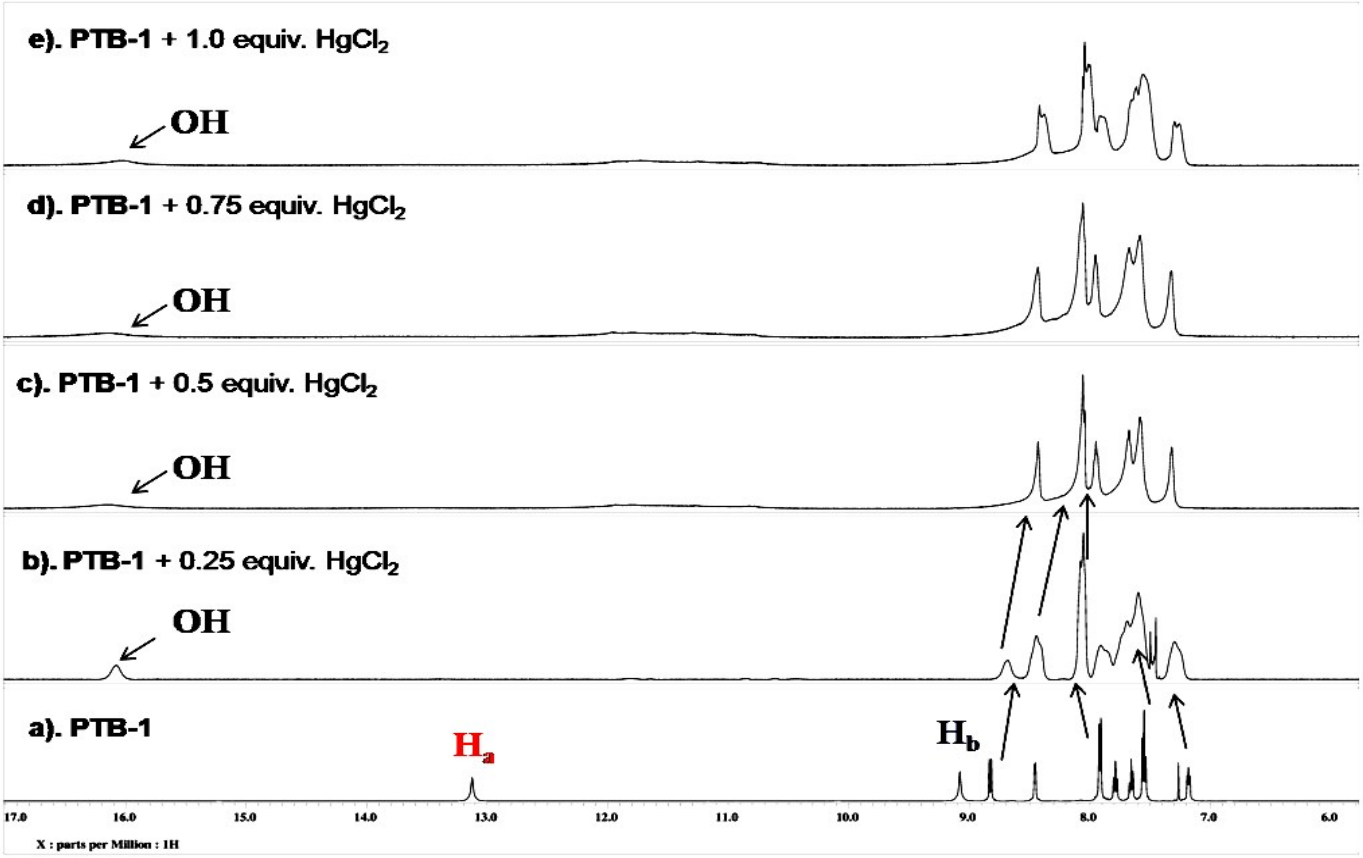

Figure S-17: Partial ^{1}H NMR spectra (aromatic region) of receptor **PTB-1** (a), **PTB-1** in the presence of 0.25 equiv. $HgCl_2$ (b), 0.5 equiv. $HgCl_2$ (c) and 1.0 equiv. $HgCl_2$ (d) taken in $CDCl_3$.

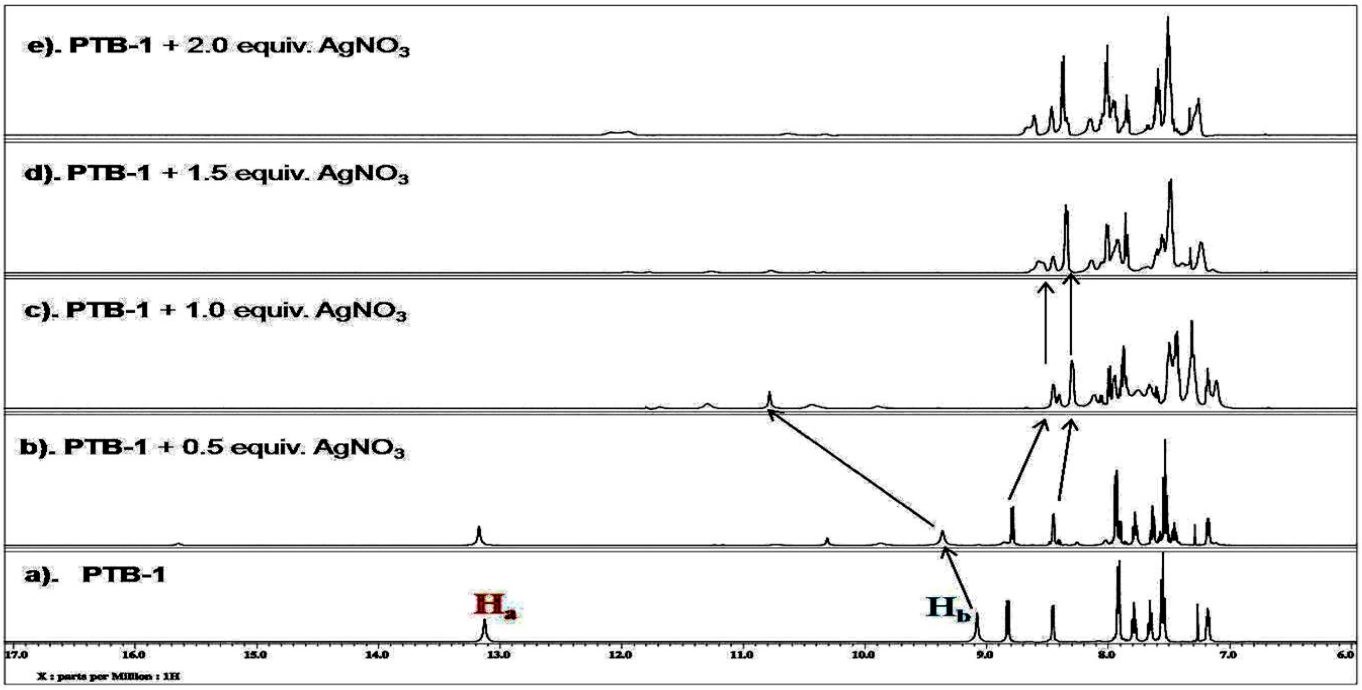

Figure S-18: Partial ^{1}H NMR spectra of receptor **PTB-1** (a), **PTB-1** in the presence of 0.5 equiv. $AgNO_3$ (b), 1.0 equiv. $AgNO_3$ (c), 1.5 equiv. $AgNO_3$ (d) and 2.0 equiv. $AgNO_3$ (e) taken in $CDCl_3$.

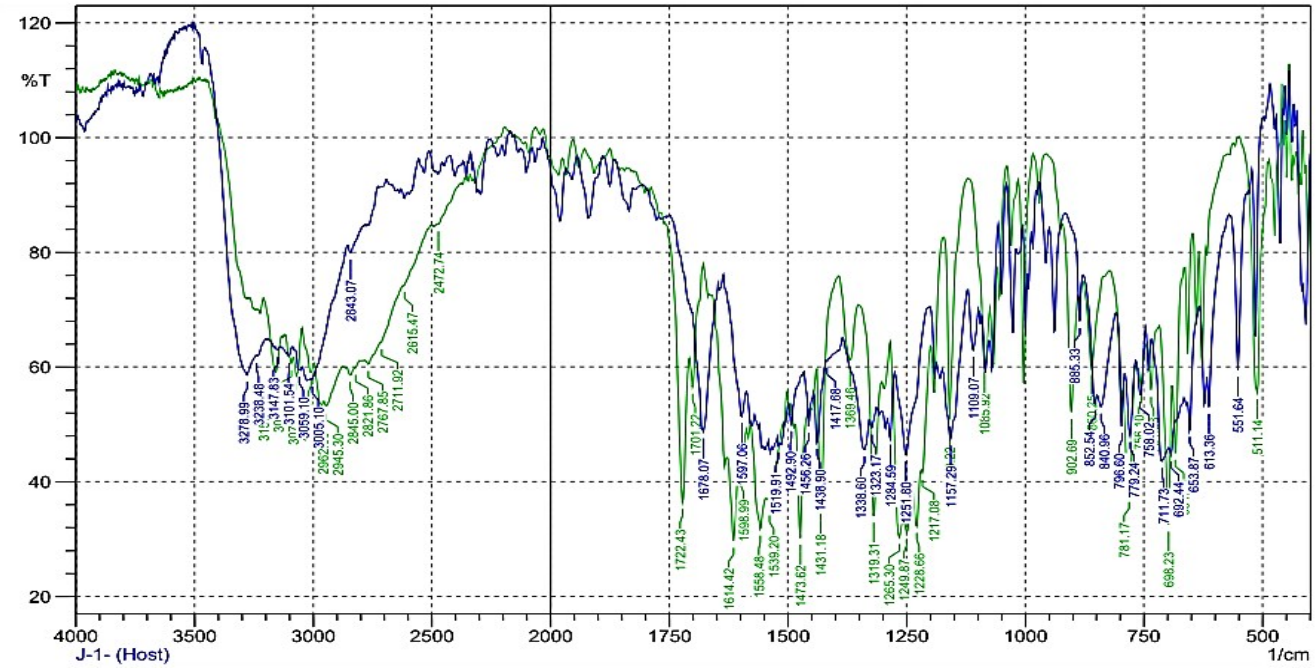

Figure S-19: FT-IR overlap spectra of **PTB-1** (blue color) and **PTB-1**+Hg^{2+} complex (green color).

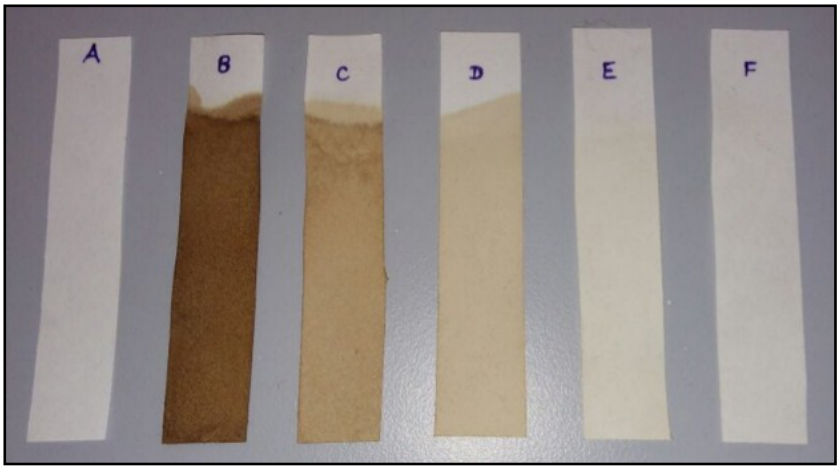

Figure 20: Photographs of PTB-1 loaded test strips with varying concentration of Ag^{+}

A= PTB-1 ($1x10^{-2}$ M) loaded test strip and [Ag^{+}] : B = 1 x 10^{-4} M, C = 5 x 10^{-5} M, D = 1 x 10^{-5} M, E = 5 x 10^{-6} M, F = 1 x 10^{-6} M

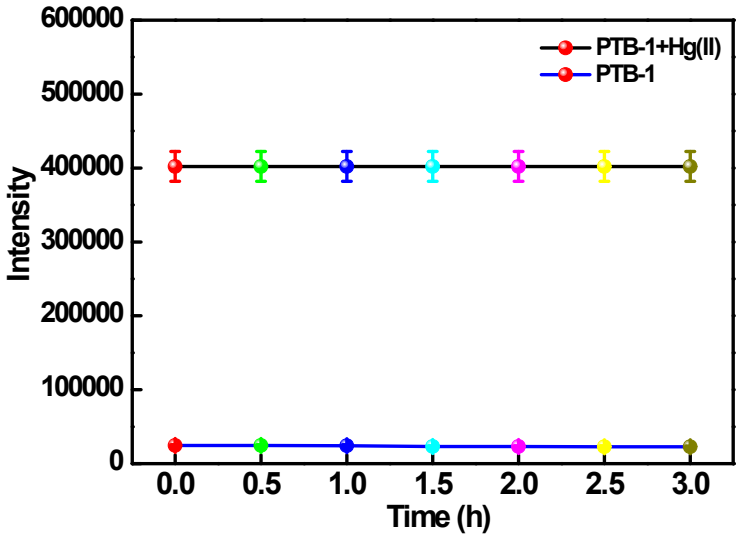

Figure S21: Fluorescence stability of PTB-1 [(2 mL, 4 x 10^{-5} M) in CH_3OH:H_2O (20:80, v/v)] upon 0 - 3 h. λ_{ex} = 290 nm, λ_{em} = 420 nm. The data were shown as mean (± s.d.) (n = 7).

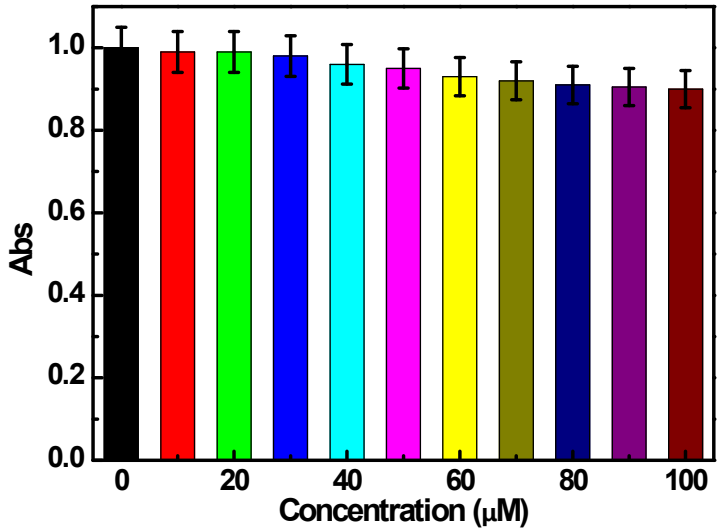

Figure S22: MTT assay of HepG2 cells with different concentrations of PTB-1. The data were shown as mean (± s.d.) (n = 7).

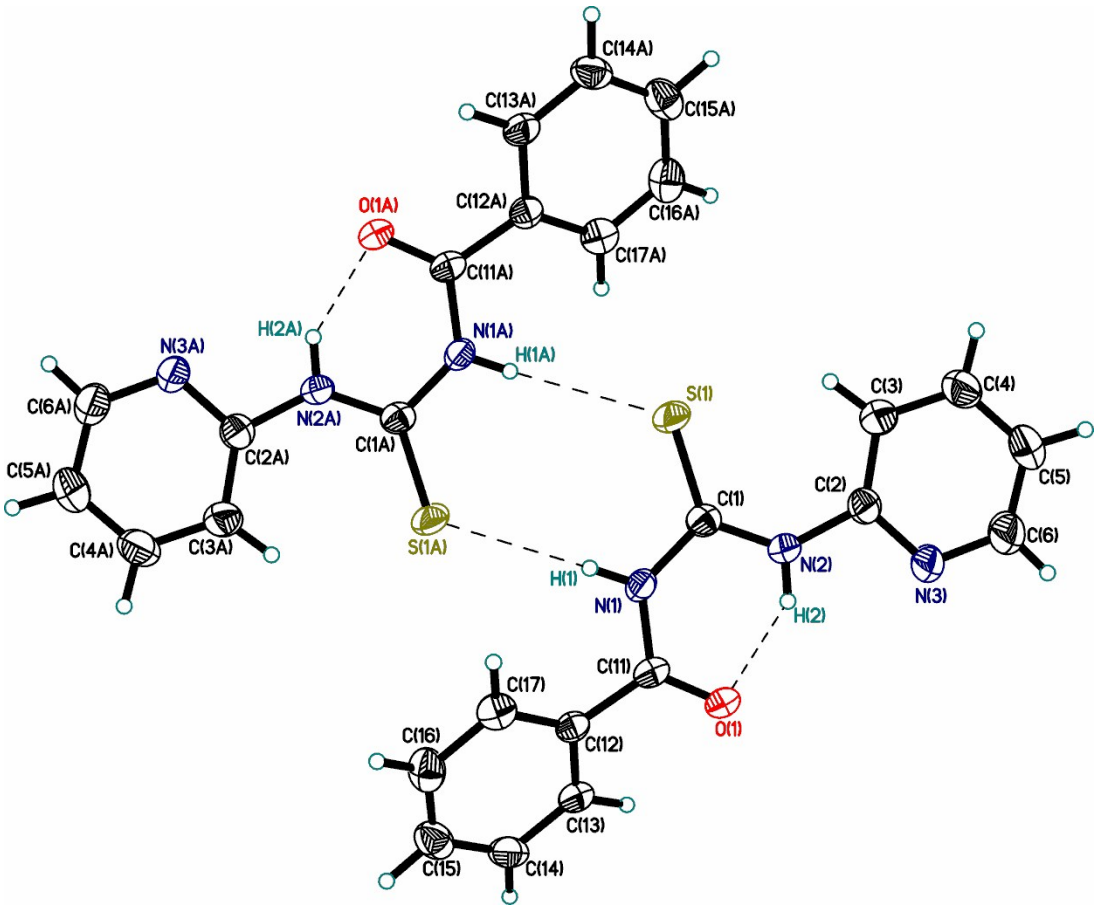

Figure S-23: Hydrogen-bonded centrosymmetric dimers in the structure of **PTB-1**.

Table S-1 Comparison of **PTB-1** with previously reported sensors.

Research Group	**Selectivity for**	**Solvent for analysis**	**Detection limit**	**Application**
Patil, U.D. *et. al.* (This paper)	Ag^{+} and Hg^{2+}	Methanol:water (20:80)	For Ag^{+} : 3.67 x 10^{-6} M For Hg^{2+}: 0.69 x 10^{-9} M	Cell Imaging, Paper Strips, Supported Silica
Fu, Y. *et. al.*	Only Ag^{+}	THF:water (80:20)	2.92 x 10^{-7}M and 6.5 x 10^{-7} M	--
Hatai, J. *et. al.*	Only Hg^{2+}	Methanol:water (80:20)	1.03 x 10^{-7} M	--
Hatai, J. *et. al.*	Only Ag^{+}	DMSO:water (1:99)	1.0 x 10^{-7} M	Cell Imaging, Paper Strips
Hu, Z.Q. *et. al.*	Only Hg^{2+}	Ethanol:water (11:89)	4.2 x 10^{-8} M	Cell Imaging
Mahapatra, A.K. *et. al.*	Only Hg^{2+}	Acetonitrile:water (20:80)	4.0 x 10^{-7} M	Cell Imaging
Tang, B. *et. al.*	Only Hg^{2+}	Acetonitrile	1.39 x 10^{-8} M	Cell Imaging
Vedamalai, M. *et. al.*	Only Hg^{2+}	Acetonitrile:water (90:10)	0.226 x 10^{-6} M	Cell Imaging
Wang, Y. *et. al.*	Only Ag^{+}	Ethanol:water (10:90)	2.79x10^{-7} M	--
Xiang, G. *et. al.*	Only Ag^{+}	THF	5 x 10^{-8} M	--
Ye, J.H. *et. al.*	Only Ag^{+}	THF:water (33:66)	0.2 x 10^{-6} M	--
Zhang, D. *et. al.*	Only Hg^{2+}	Ethanol:water (50:50)	0.067 x 10^{-6} M	Cell Imaging
Zheng, H. *et. al.*	Only Ag^{+}	Methanol:water (20:80)	34 x 10^{-9} M	--

References

Fu, Y., Mu, L., Zeng, X., Zhao, J.L., Redshaw, C., Ni, X.L., Yamato, T., 2013. J. Chem. Soc., Dalton Trans. 42, 3552-3560.

Hatai, J., Pal, S., Bandyopadhyay, S., 2012. RSC Adv. 2, 10941-10947.

Hatai, J., Pal, S., Jose, G.P., Bandyopadhyay, S., 2012. Inorg. Chem. 51, 10129-10135.

Hu, Z.Q., Zhuang, W.M., Li, M., Liu, M.D., Wen, L.R., Li, C.Z., 2013. Dyes Pigments 98, 286-289.

Mahapatra, A.K., Maji, R., Sahoo, P., Nandi, P.K., Mukhopadhyay, S.K., Banik, A., 2012. Tetrahedron Lett. 53, 7031-7035.

Tang, B., Cui, L.J., Xu, K.H., Tong, L.L., Yang, G.W., An, L.G., 2008. ChemBioChem 9, 1159-1164.

Vedamalai, M., Wu, S.P., 2012. Org. Biomol. Chem.10, 5410-5416.

Wang, Y., Geng, F., Xu, H., Qu, P., Zhou, X., Xu, M., 2012. J. Fluoresc. 22, 925-929.

Xiang, G., Cui, W., Lin, S., Wang, L., Meier, H., Li, L., Cao, D., 2013. Sens. Actuators, B 186, 741-749.
Ye, J.H., Duan, L., Yan, C., Zhang, W., He, W., 2012. Tetrahedron Lett. 53, 593-596.
Zhang, D., Li, M., Jiang, Y., Wang, C., Wang, Z., Ye, Y., Zhao, Y., 2013. Dyes Pigments 99, 607-612.
Zheng, H., Yan, M., Fan, X.X., Sun, D., Yang, S.Y., Yang, L.J., Li, J.D., Jiang, Y.B., 2012. J. Chem. Soc., Chem. Commun. 48, 2243-2245.